Longitudinal Beam Dynamics Simulations for the 16 GeV Proton Driver

A. A. Kepley

Case Western Reserve University

10900 Euclid Ave., Cleveland, OH 44106

Supervisor: C. M. Bhat

Fermi National Accelerator Laboratory *

P.O. Box 500, Batavia, IL 60510

(August 5, 1999)

Abstract

The recently proposed Proton Driver would increase the present Booster intensity by a factor of twenty to the intensity needed for future high energy physics research programs at Fermilab. The purpose of this paper is to study the single particle longitudinal beam dynamics of the 16 GeV Booster component of the Proton Driver using both a real and an imaginary γ_{tr} lattice. Since ESME simulations using the initial design parameters for the Booster indicated that particles were lost early in the acceleration cycle, we systematically varied the longitudinal emittance, initial rf voltage, and bunch intensity looking for values of these quantities which would provide acceleration without particle loss. From our simulations, we found that space charge forces play a very important role at the beginning of acceleration. Our simulations

*Operated by the Universities Research Association, under contract with the U.S. Department of Energy

also show that the imaginary γ_{tr} lattice ($\gamma_{tr} = 26i$) is the more cost effective lattice because it was able to accelerate particles successfully using a lower rf voltage than the real γ_{tr} lattice ($\gamma_{tr} = 26$).

I. INTRODUCTION

An upgrade of the current Proton Source is vital for the expansion of Fermilab's high energy physics program. The bunch intensity from the present 8 GeV Booster and 400 MeV Linac is barely enough to support ongoing Fermilab projects and is certainly inadequate for future high energy physics research programs. The recently proposed upgrade to the Proton Source, the Proton Driver, would initially be composed of a new 16 GeV Booster. A 1 GeV Linac and a 3 GeV Pre-Booster would be added on later along with upgrades to the 16 GeV Booster [1–3]. In its final form, the Proton Driver would increase the present Booster intensity by a factor of twenty and would help to increase the luminosity in the Tevatron and in fixed target experiments, like the neutrino oscillation experiment known as MiniBooNE, as well as in the muon collider. This paper will focus on the 16 GeV Booster component of the Proton Driver, referred to here as the 16 GeV Proton Driver or the Booster.

The 16 GeV Proton Driver would be a proton synchrotron accelerator. Two different lattice types have been proposed for this machine. The first would produce a transition energy of about 26 GeV, which would be much higher than the extraction energy of the Booster, and the second would produce an imaginary transition energy, the value of which has yet to be determined. The advantage of both these arrangements is that they allow the Booster to avoid the problems caused by transition crossing—one by extracting the beam well before it would reach transition and the other by making it impossible for the beam to encounter transition [4].

The purpose of this paper is to use the program ESME to model the longitudinal beam dynamics of the 16 GeV Proton Driver using both real and imaginary transition energies. Section II of this paper will present some theoretical background on proton synchrotrons,

longitudinal dynamics, and longitudinal instabilities. Section III will give more information on the program ESME and the specifics of our simulation. Our results along with a discussion of their meaning will be presented in section IV. Finally in section V, we will give our conclusions about the 16 GeV Proton Driver design parameters, concentrating on the differences between real and imaginary transition energies.

II. THEORY

A. Proton Synchrotrons

A proton synchrotron has four major components: dipole magnets which guide the particles into a closed orbit, quadrupole magnets which focus the beam of particles, a connecting vacuum beam pipe which reduces particle loss caused by the collision of the particle beam with air molecules, and radio frequency (rf) cavity system which bunches the particles or changes the energy of the particles. If the energy of the particles is being changed, the dipole and quadrupole fields must be varied with the energy of the particles in order to keep the beam in a closed orbit. The momentum of a particle, p, the dipole magnetic field strength, B, and the radius of a circular accelerator, R, are related through the equation

$$p = \frac{eBR}{c}. \tag{2.1}$$

Since particles in a synchrotron go through the same rf cavity many times, synchrotrons are able to accelerate particles to very high energies in a more cost efficient manner than other types of accelerators. [5,6]

B. Longitudinal Beam Dynamics

Following reference [5], the voltage, $\hat{V}$, in the rf cavity of a proton synchrotron varies like

$$V(t) = \hat{V} \sin \phi(t), \tag{2.2}$$

where $\phi(t)$ is the phase of the rf voltage. Due to the sinusoidal variation of the rf voltage, a particle must arrive in the rf cavity at the right time in the voltage cycle to be accelerated by the desired amount. The particle that accomplishes this feat is called the synchronous particle. The energy gain per turn, dE, of the synchronous particle is given by

$$dE = e\hat{V} \sin \phi_s, \tag{2.3}$$

where ϕ_s is the phase of the synchronous particle. The phase of a particle is related to the azimuthal angle around the machine, θ, by the equation

$$\phi = -h\theta, \tag{2.4}$$

where h is the harmonic number of the voltage source. The negative sign is a convention indicating that the particle is traveling in the $+\theta$ direction around the synchrotron. From equation 2.4, the angular frequency of the rf cavity, ω_{rf}, is related to the revolution frequency of the synchronous particle, ω_s, by

$$\omega_{rf} = h\omega_s, \tag{2.5}$$

where ω_s is

$$\omega_s = \frac{\beta_s c}{R}. \tag{2.6}$$

As noted previously, the synchronous particle arrives in the rf cavity at exactly the right time to receive exactly the right amount of energy to be properly accelerated. What happens to the other particles in the synchrotron? If the particle has slightly more energy than the synchronous particle, it arrives at the rf cavity sooner than the synchronous particle, as does particle A in figure 1. From the voltage curve in figure 1, one can see that particle A, which had more energy than the synchronous particle B going into the rf cavity, will receive less energy from the rf cavity than particle B. Therefore, particle A will slow down with respect to particle B. Alternately, a particle that arrives at the rf cavity a short while after the synchronous particle, like particle C in figure 1, had less energy than the synchronous

particle going into the rf cavity, but will receive more energy in the rf cavity than the synchronous particle. This extra energy will make particle C speed up with respect to particle B. Let's say that particle C now has the most energy and particle A now has the least energy. Then the next time through the rf cavity particle C will be slowed down with respect to the synchronous particle and particle A will be speeded up with respect to the synchronous particle. Now, as at the beginning of this example, particle A has the most energy and particle C has the least energy and the whole cycle repeats itself. This oscillation of particles in energy and time space is called synchrotron oscillation. The presence of stable synchrotron oscillations about a synchronous energy for particles relatively close the synchronous particle is referred to as phase stability. Phase stability in turn leads to phase focusing or the tendency for particles to form clusters called bunches. The synchrotron oscillation frequency, Ω_s, is given by

$$\Omega_s = \left(-\frac{eV\eta\omega_s \cos\phi_s}{2\pi pR} \right)^{\frac{1}{2}}, \tag{2.7}$$

where $\eta = \gamma_{tr}^{-2} - \gamma_s^{-2}$ and γ_{tr} is the transition energy. The ratio of the synchrotron oscillation frequency to the revolution frequency of the synchronous particle is called the synchrotron oscillation tune. [5,6]

The equations of motion for particles in a proton synchrotron can be obtained from the Hamiltonian

$$H(q,y) = \frac{1}{2}\omega_{rf}^2 \frac{\eta}{\beta^2 E_s} y^2 + \frac{eV}{2\pi h}\left[\Gamma q + \cos(q+\phi_s)\right], \tag{2.8}$$

where $q = \phi - \phi_s$, $y = \frac{(E-E_s)}{w_{rf}}$, $\Gamma = \sin\phi_s$, and E_s is the energy of the synchronous particle. Analysis of this equation in q-y phase space reveals two main areas of particle motion: one in which the energy of the particles undergoes stable oscillations about a synchronous energy, i.e., energy of a synchronous particle, and another in which these oscillations are unstable. The curve bounding stable region is called the separatrix and is given by the equation

$$A\frac{y^2}{2} + B\left(\Gamma\phi + \cos\phi - \Gamma\phi_1 - \cos\phi_1\right) = 0, \tag{2.9}$$

where $A = \omega_{rf}^2 \frac{\eta}{\beta^2 E_s}$, $B = \frac{eV}{2\pi h}$, and $\phi_1 = \pi - \phi_s$. The stable region is referred to as a bucket. The number of buckets in a ring is the same as the harmonic number of the rf source. If ϕ_s is 0 or π, the bucket is not accelerating and is called a stationary bucket. For all other values of ϕ_s between 0 and 2π, the bucket is either accelerating or decelerating and is called a moving bucket. The phase space area of a stationary bucket is

$$S = 16 \left(\frac{B}{|A|} \right)^{\frac{1}{2}} [eV - sec] \tag{2.10}$$

and the phase space height is

$$Y_b = 2 \left(\frac{B}{|A|} \right)^{\frac{1}{2}} [eV - sec]. \tag{2.11}$$

The phase space area of a bunch of particles, also called its longitudinal emittance, is

$$\epsilon_l = 16 \left(\frac{B}{|A|} \right)^{\frac{1}{2}} \frac{\pi}{64} \Delta^2 \left(1 - \frac{5}{384} \Delta^2 \right), \tag{2.12}$$

where the bucket is stationary and Δ is the total bunch length in radians. [8] Finding the phase space area and height of a moving bucket and the longitudinal emittance of the beam inside that bucket is much more difficult. The reader should consult reference [7] for further information.

Transition energy, γ_{tr}, is a major concern in proton synchrotron design. When the energy of a particle is below transition energy, an increase in energy means an increase in velocity. Above transition energy, however, the particle's velocity is very close to the speed of light so an increase in energy manifests as an increase in mass according to $E = mc^2$. In general terms, this means that prior to transition a higher energy particle will have a higher frequency than a lower energy particle, but that after transition a higher energy particle will have a lower frequency than a lower energy particle. Thus particles with two different initial energies, but essentially the same frequency, may arrive at the rf cavity at the same time and receive the same amount of energy, rather than receiving different amounts of energy. The frequency slip factor

$$\eta = \gamma_{tr}^{-2} - \gamma_s^{-2} \tag{2.13}$$

gives the deviation of the revolution period of a non-synchronous particle from the revolution period of the synchronous particle. When η is less than zero the particle is below transition, when η is greater than zero the particle is above transition, and when η equals zero the particle is at transition. The acceleration of particles through transition disturbs phase stability and the bunch becomes highly unstable. To avoid this problem altogether one can configure the machine's magnets either to give an imaginary transition energy or to produce a γ_{tr} higher than the machine's maximum energy [4].

C. Longitudinal Instabilities

Beam loss and unwanted emittance growth can disrupt the ideal operation of a proton synchrotron. These problems can be attributed to the effects of longitudinal instabilities caused by space charge forces and beam image current to name a few culprits. For more information on other longitudinal instabilities, please consult reference [6]. Space charge forces are the repulsive electrical forces between similarly charged particles. Proton synchrotrons use magnets and rf cavities to force similarly charged particles to move closer together. If the magnetic field and/or the rf voltage is not strong enough to overcome the repulsive electrical forces among the protons in a bunch, space charge forces can cause an increase in longitudinal emittance. This effect can be modeled using the equation [9]

$$\left(\frac{Z_{||}}{n}\right)^{space-charge} = \frac{377}{2\beta\gamma^2}\left(1 + 2\ln\frac{b}{a}\right) i[Ohm] \tag{2.14}$$

where b is the average beam pipe radius and a is the average beam size. Beam image current is produced by the interaction of beam with the conducting beam pipe wall. Since the flow of the image current opposes the flow of the beam current, an impedance is created. This impedance can be modeled using the broadband impedance form of the general resonator equation

$$Z_{||}(\omega) = \frac{R_S}{\left[1 + i\left(\frac{\omega_R}{\omega} - \frac{\omega}{\omega_R}\right)\right]}, \tag{2.15}$$

where R_S is the shunt impedance in ohms and the resonance angular frequency, ω_R, is equal to $2\pi f_R$ [9].

III. SIMULATION DETAILS

A. ESME

The longitudinal beam dynamics of the 16 GeV Booster were modeled using the program ESME [10]. This program tracks particles using a pair of difference equations [11]

$$\Theta_{i,n} = \left[\frac{\tau_{s,n-1}}{\tau_{s,n}} \Theta_{i,n-1} + 2\pi \left(\frac{\tau_{i,n}}{\tau_{s,n}} - 1 \right) \right] \tag{3.1}$$

$$E_{i,n} = \left[E_{i,n-1} + eV(\phi_{s,n} + h\Theta_{i,n}) - eV(\phi_{s,n}) \right], \tag{3.2}$$

where s denotes the synchronous particle, i denotes a non-synchronous particle, n is the turn number, and τ is the period. The input for this program consists of ring parameters such as the radius of the synchrotron and the initial and final kinetic energy of the synchronous particle, rf parameters such as harmonic number and maximum voltage, and bunch properties such as longitudinal emittance and distribution. Impedance, resonance, and space charge effects can also be added to the simulation. The output consists of a great variety of graphs and some text on the run. We used the esme2000 version of this program which was modified by J. MacLachlan to include imaginary γ_{tr}.

B. Proton Driver Specifications

The design specifications for the 16 GeV Proton Driver at each stage of construction are given in table I. As of the writing of the paper, complete specifications for this machine had not yet been finalized, but a design team was working to complete a Technical Design Report for the Proton Driver by the end of FY 2000. Figure 2 depicts the setup of the first stage Booster. The parameters for the 16 GeV Booster used in our simulations are given

in table II. Since there was such a wide variation in rf frequency (from 37.9 to 53.0 MHz), broadband impedance values were calculated at four different times in the cycle in order to more accurately model this impedance. See table III for more information. As mentioned in the introduction, we used both 26 and $26i$ for the transition energy in order to compare their effects on the acceleration cycle. The magnetic field ramp was calculated from the function [12]

$$B(t) = B_i + (B_f - B_i)\left(-\frac{\cos(\pi(x+a)) - b\cos(2\pi(x+c)) + \cos(\pi a) + b\cos(2\pi c)}{2\cos(\pi a)}\right), \quad (3.3)$$

where B_i and B_f are the initial and final magnetic fields, x is a normalized time variable, and the constants a, b, and c can be adjusted to give the desired ramp shape. The constant a gives the magnetic ramp an initial slope, constant b adds a second rf harmonic, and constant c changes the phase of the second harmonic in relation to the first harmonic. In our simulations, a was 2, b was 0.12, and c was 0.25. The acceleration ramp, i.e., the momentum of the synchronous particle as a function of time, can be obtained by using equations 2.1, 3.3, and

$$E^2 = p^2 + m_o^2 c^4. \quad (3.4)$$

Figure 3 shows acceleration ramp used in our simulations.

IV. RESULTS AND DISCUSSION

Neglecting space charge forces and broadband impedance effects, the ESME simulation of the 16 GeV Proton Driver was able to model the Booster acceleration cycle without losing any particles. With the inclusion of broadband impedance effects, the simulation continued to show no particle loss. Once space charge forces were added to the simulation, however, particle loss was seen in the ESME output; about 0.92% of the particles were lost using imaginary transition energy and about 2.4% of the particles were lost using real transition energy. Since the given parameters did not accelerate the bunch successfully, i.e., without

losing any particles, we varied the longitudinal emittance, initial rf voltage, and bunch intensity looking for values of these quantities that produced a successful acceleration simulation. All other quantities were kept at their design values. Both real and imaginary transition energies were used in these simulations. Since most of the particle loss in our simulations occurred during the first quarter of the simulation, only this part of the simulation needed to be examined in order to determine if the entire simulation was successful.

Figures 4 and 5 show regions of successful acceleration for the first quarter of the simulation where both intensity and longitudinal emittance were varied and the initial rf voltage was 1.23 MV. Note that these regions appear to be the same for both values of γ_{tr} and that the initial rf voltage design value was only able to accelerate very low bunch intensities successfully. The regions of successful acceleration for the first quarter of the simulation where longitudinal emittance and initial rf voltage were varied and the bunch intensity was 3×10^{11} ppb are shown in figures 6 and 7. Again, the regions of successful acceleration appear to be the same for both values of γ_{tr}. From these figures, one can see that much higher voltages, ranging from about 2.5 MV to about 4.0 MV, were needed to accelerate the design intensity successfully. In figures 8 and 9, where the initial rf voltage and bunch intensity were varied and the longitudinal emittance was 0.03 eV-sec, the regions of stable acceleration for imaginary and real transition energies differ, although there are some structural similarities between the regions. In these graphs, however, the trend of needing high rf voltages to successfully accelerate large bunch intensities continues.

The values of longitudinal emittance, initial rf voltage, and intensity to be run through the entire simulation were selected from the stable regions in figures 4 through 9. Surprisingly, when parameters were picked from the edges of the identical regions of stability in figures 4 through 7, the simulation using real transition energy often lost particles while the simulation using imaginary transition energy did not. A striking example of this phenomenon was seen with an initial voltage of 2.5 MV, a longitudinal emittance of 0.04 eV-sec, and an intensity of 3×10^{11} ppb. From figures 6 and 7 one can see that these values are in the stable region for the first part of the simulation for both imaginary and real transition

energy. In full length simulations, however, the simulation using a real transition energy lost 0.006% of its particles while the simulation using an imaginary transition energy lost none. In general, full length simulations with real transition energy using parameters from the edge of the region of stability seemed to lose particles, while full length simulations with imaginary transition energy did not.

Two full length simulations using the best parameters for imaginary and real transition energy can be seen in figures 10 and 11. When comparing these two simulations, note that the particles in the imaginary transition energy simulation were successfully accelerated using a much lower voltage than the real transition energy case (2.5 MV rather than 4.0 MV). The emittance of the bunch in the imaginary transition energy situation also increased at a slower pace and had a smaller final value than in the real transition energy situation. In the imaginary transition energy case, however, the synchrotron oscillation tune had much larger values than in the real transition energy case.

V. CONCLUSIONS

Longitudinal instabilities, especially those due to space charge forces, are major concerns for high intensity, low emittance proton synchrotrons. Our longitudinal beam dynamics simulations of the 16 GeV Proton Driver, including space charge forces and broadband impedance, indicated that proton synchrotrons with an imaginary transition energy needed approximately 40% less initial rf voltage than proton synchrotrons with a real transition energy. The simulations using imaginary transition energy, however, had larger synchrotron tunes which may cause problems with other aspects of the accelerator. After surveying possible values for the intensity, longitudinal emittance, and initial voltage, we found that the best values for acceleration in the 16 GeV Proton Driver were an intensity of 3×10^{11} ppb, a longitudinal emittance of 0.04 eV-sec, an initial rf voltage of 2.5 MV, and a transition energy of $26i$ GeV. If a real transition energy of 26 GeV is stipulated, the voltage requirement increases to 4.0 MV. Since the best initial voltage we found was approximately twice the

design specification of 1.23 MV, our results indicate that further investigation into the rf system and the lattice for the 16 GeV Proton Driver needs to be undertaken in order to design the most useful and cost-efficient proton synchrotron possible.

VI. ACKNOWLEDGMENTS

I am indebted to a great many people for their direct and/or indirect help with this project. Nevertheless, I have managed to single out three parties who deserve especial recognition. First of all, I would like to thank Dr. Bhat for his patience with me as I learned what I needed to know to get this project off the ground, for his revision of innumerable drafts of my paper, and for many helpful discussions along the way. I would also like to thank Dr. MacLachlan for his invaluable aid in revising ESME to include imaginary transition energy in the longitudinal beam dynamics simulations as well as for many helpful conversations. Finally, my deep appreciation and gratitude goes out to the SIST committee for selecting me to participate in this wonderful program.

REFERENCES

[1] Holmes, S.D., ed. "A Development Plan for the Fermilab Proton Source." Fermilab publication TM-2021, September 1997.

[2] Chou, Weiren. "Status of the Proton Driver Study at Fermilab." Fermilab pre-print Conf-99/104, May 1999.

[3] Raja, Rajendran, ed. "Muon Colliders: A scenario for the evolution of the Fermilab accelerator complex." Fermilab Director's Report, http://www-d0.fnal.gov/~raja/dirrep.ps, accessed on June 29, 1999.

[4] Lee, S.Y., K.Y. Ng, and D. Trbojevic. "Design and Study of Accelerator Lattices without Transition." Fermilab pre-print, FN-595, October 1992.

[5] Weng, W. T. "Fundamentals of Longitudinal Motion." In *AIP Conference Proceedings 184*, Vol. 1. Eds. Melvin Month and Margaret Dienes. New York: American Institute of Physics, 1989, pp. 243-287.

[6] Edwards, D.A. and M.J. Syphers. *An Introduction to the Physics of High Energy Accelerators.* New York: John Wiley and Sons, Inc., 1993.

[7] Ohnuma, S. "The Beam and the Bucket: A Handbook for Analysis of Longitudinal Motion." Fermilab publication, TM-1381, January 22, 1986.

[8] Martin, Philip S. and Sho Ohnuma. "Longitudinal Phase Space in Circular Accelerators." In *AIP Conference Proceedings 184*, Vol. 2. Eds. Melvin Month and Margaret Dienes. New York: American Institute of Physics, 1989, pp. 1941-1968.

[9] Rivera-Medero, F. and C.M. Bhat. "Coupled-bunch instability in the Fermilab Main Injector: Longitudinal-phase-space simulation." Fermilab SIST Program Final Report, August 1998.

[10] MacLachlan, J. and J.F. Ostiguy. "Enhancements to the Longitudinal Dynamics Code

ESME." Fermilab pre-print conf-97-168, May 1997.

[11] MacLachlan, James A. "Difference Equations for Longitudinal Motion in a Synchrotron." Fermilab pre-print FN-529, December 15, 1989.

[12] MacLachlan, James A. and Jean-Francǫis Ostiguy. "User's Guide to ESME v.8.2." September 1997. http://www-ap.fnal.gov/ESME/esme-manual/esme-manual.html, accessed on July 25, 1999.

FIGURES

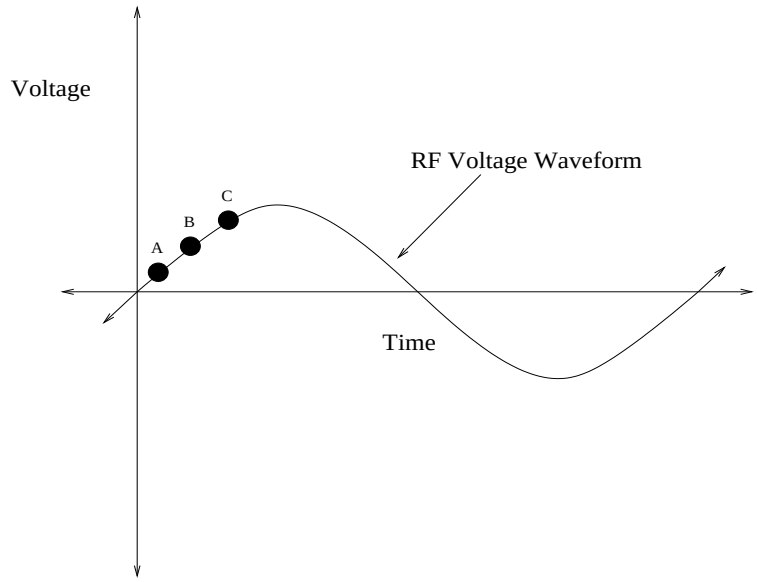

FIG. 1. RF voltage waveform demonstrating phase stability.

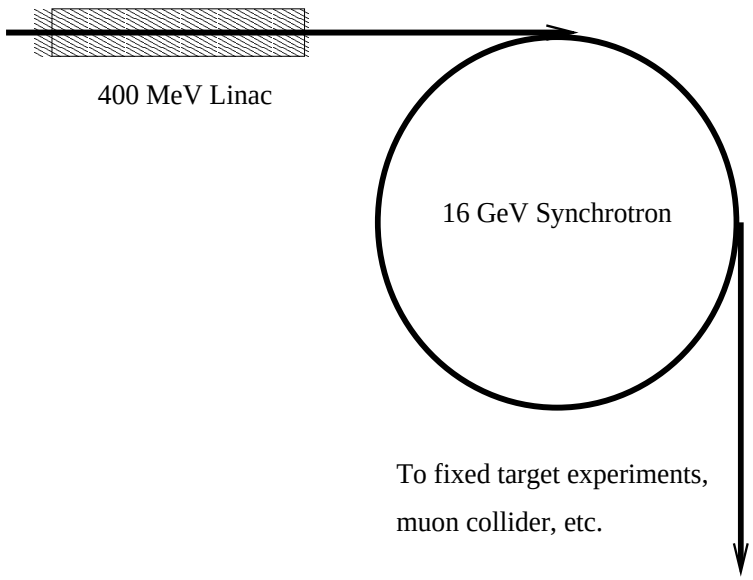

FIG. 2. A diagram of 16 GeV Booster in phase 1.

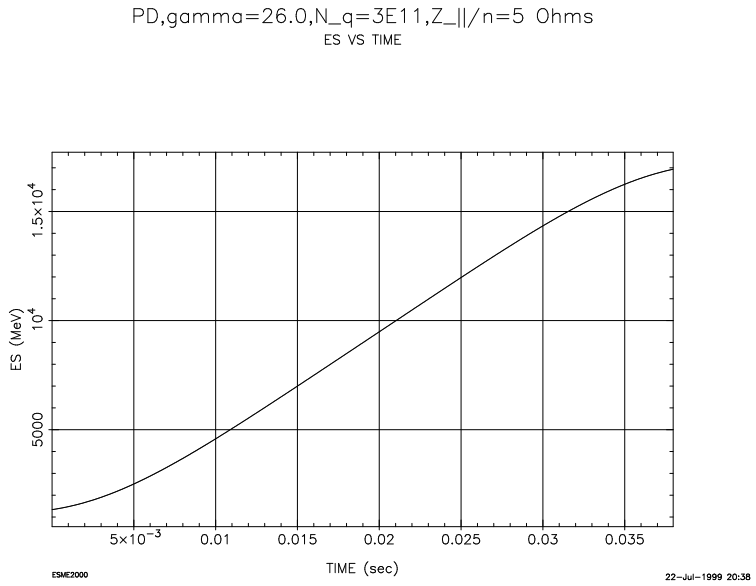

FIG. 3. Synchronous energy vs. time for the 16 GeV Proton Driver acceleration cycle used in the ESME simulations.

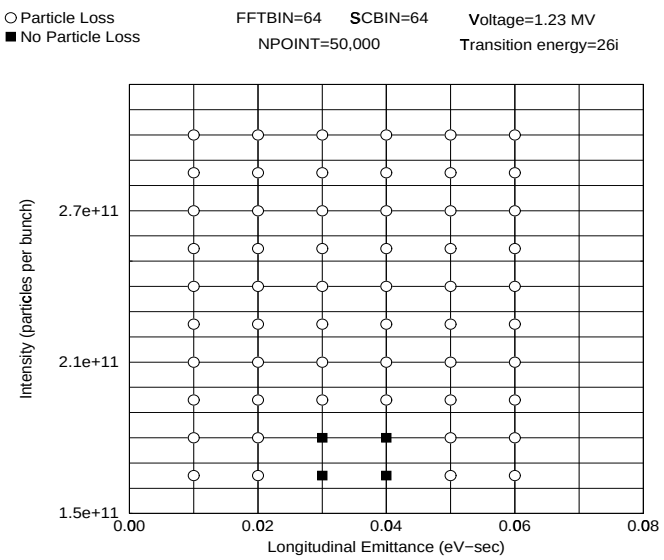

FIG. 4. Intensity vs. longitudinal emittance for $\gamma_{tr} = 26i$ showing the regions of successful particle acceleration for the first quarter of the simulation. The initial rf voltage was 1.23 MV.

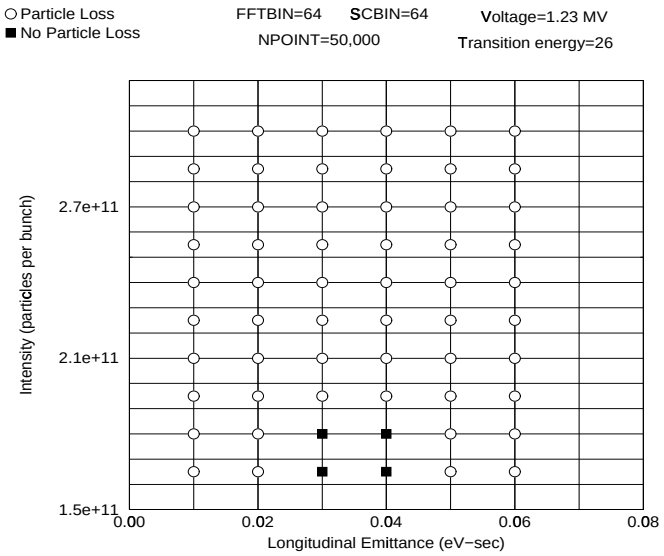

FIG. 5. Intensity vs. longitudinal emittance for $\gamma_{tr} = 26$ showing the regions of successful particle acceleration for the first quarter of the simulation. The initial rf voltage was 1.23 MV.

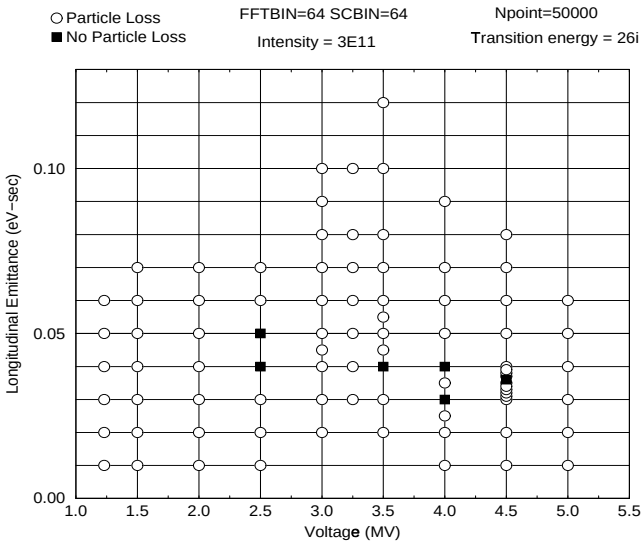

FIG. 6. Longitudinal emittance vs. voltage for $\gamma_{tr} = 26i$ showing the regions of successful particle acceleration for the first quarter of the simulation. The bunch intensity was 3×10^{11} ppb.

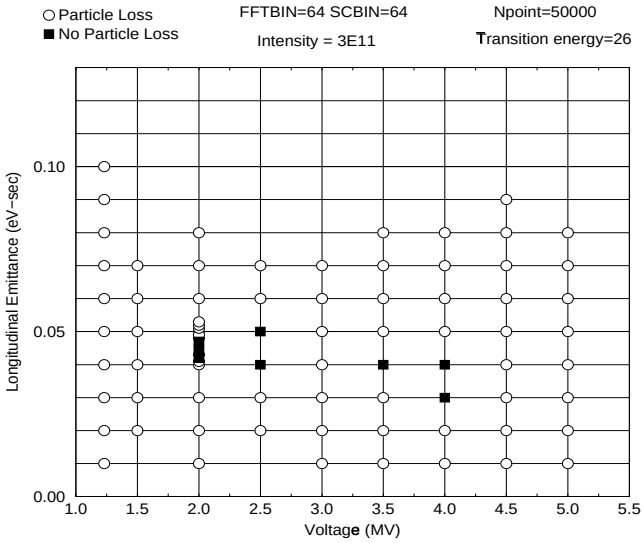

FIG. 7. Longitudinal emittance vs. voltage for $\gamma_{tr} = 26$ showing the regions of successful particle acceleration for the first quarter of the simulation. The bunch intensity was 3×10^{11} ppb.

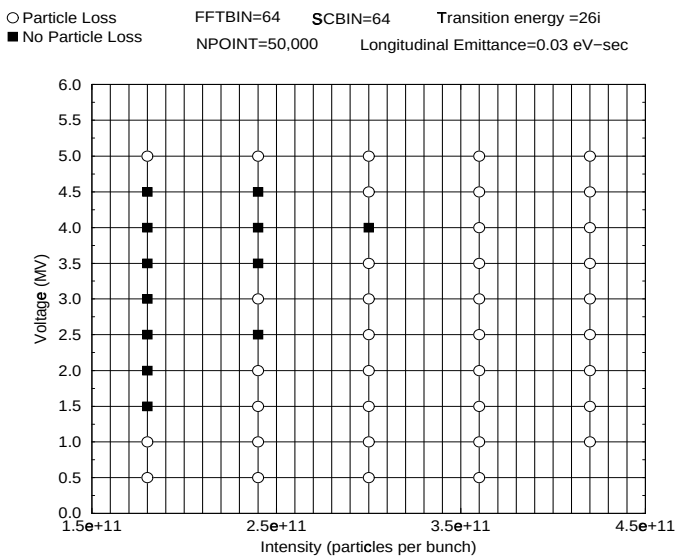

FIG. 8. Voltage vs. bunch intensity for $\gamma_{tr} = 26i$ showing the regions of successful particle acceleration for the first quarter of the simulation. The longitudinal emittance was 0.03 eV-sec.

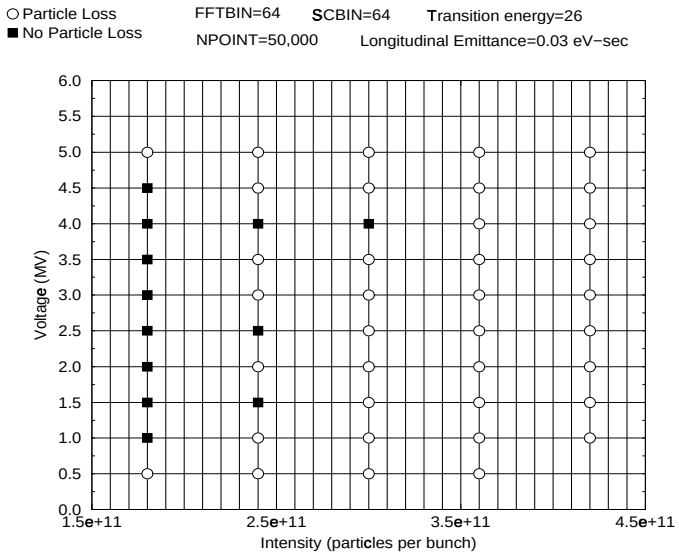

FIG. 9. Voltage vs. bunch intensity for $\gamma_{tr} = 26$ showing the regions of successful particle acceleration for the first quarter of the simulation. The longitudinal emittance was 0.03 eV-sec.

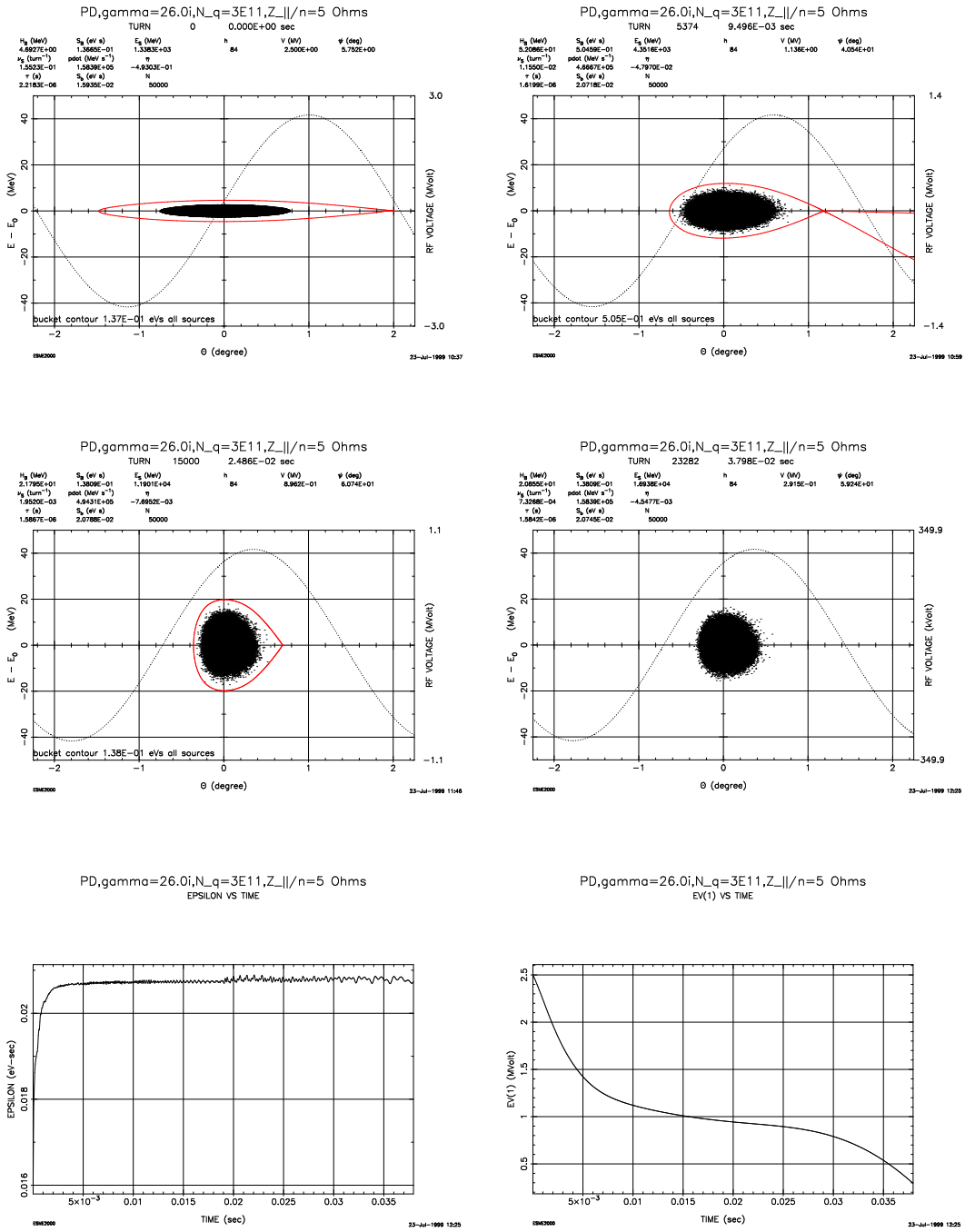

FIG. 10. *From left to right, top to bottom.* The beginning of a successful acceleration with $\gamma_{tr} = 26i$, initial voltage equal to 2.5 MV, longitudinal emittance equal to 0.04 eV-sec, and intensity equal to 3×10^{11} ppb. About a third of the way through the acceleration cycle. About two-thirds of the way through the acceleration cycle. The end of a successful acceleration. A graph of emittance vs. time. A graph of rf voltage vs. time.

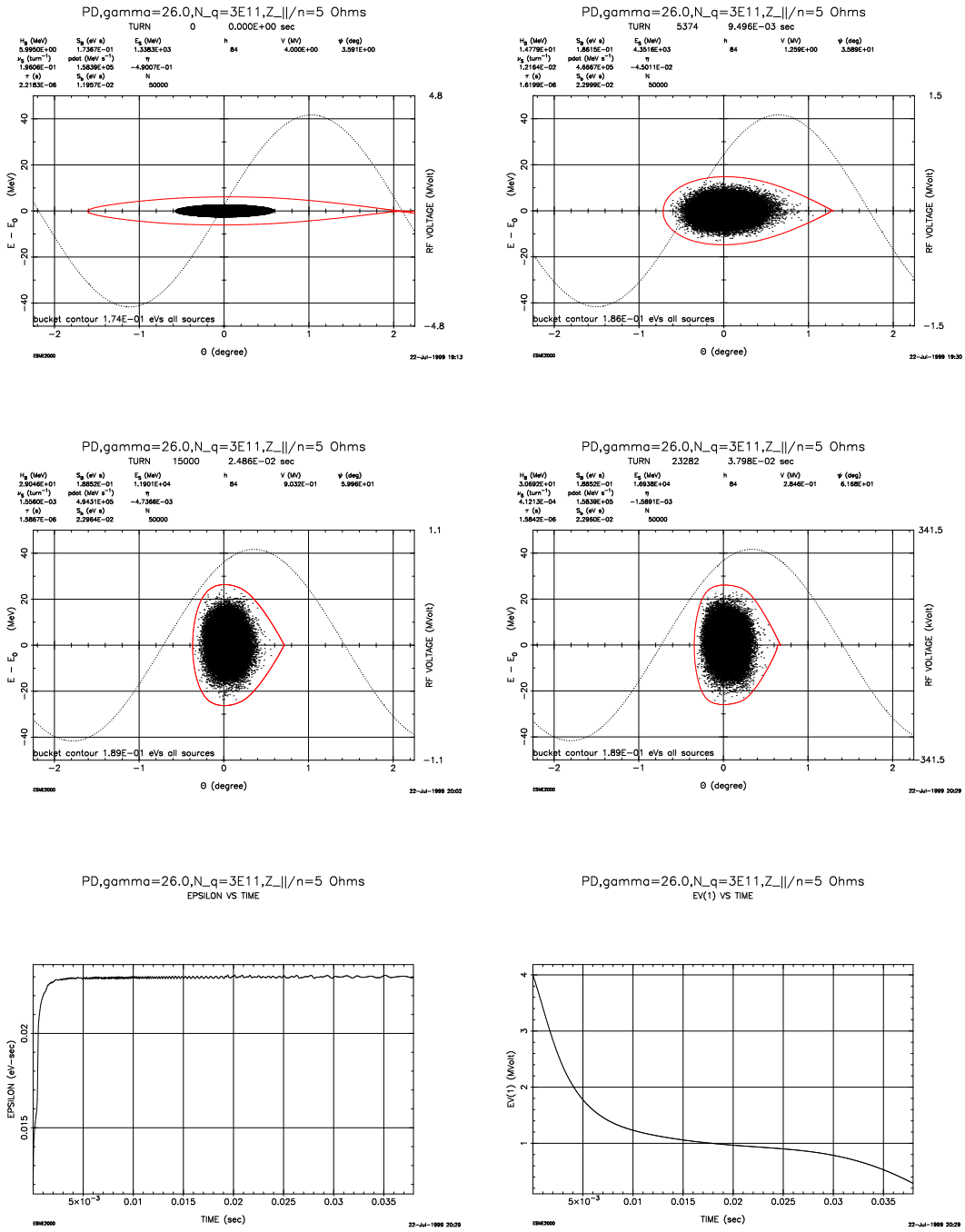

FIG. 11. *From left to right, top to bottom.* The beginning of a successful acceleration with $\gamma_{tr} = 26$, initial voltage equal to 4.0 MV, longitudinal emittance equal to 0.04 eV-sec, and intensity equal to 3×10^{11} ppb. About a third of the way through the acceleration cycle. About two-thirds of the way through the acceleration cycle. The end of a successful acceleration. A graph of emittance vs. time. A graph of rf voltage vs. time.

TABLES

TABLE I. 16 GeV Proton Driver specifications. This table was adapted from reference [3].

Booster (operating at 15 Hz)	Phase 1	Phase 2
Injection kinetic energy (GeV)	0.4	3
Extraction kinetic energy (GeV)	16	16
Protons per bunch	3×10^{11}	2.5×10^{13}
Harmonic number	84	4
Total number of protons	2.5×10^{13}	1×10^{14}
Normalized transverse emittance (mm-mrad)	50π	200π
Longitudinal emittance at injection (eV-sec)	0.03	2
Longitudinal emittance at extraction (eV-sec)	0.1	2
RF frequency (MHz)	53	7.5
Extracted bunch length (ns)	0.2	1

TABLE II. 16 GeV Proton Driver specifications used in ESME simulations.

Injection kinetic energy (MeV)	400
Extraction kinetic energy (GeV)	16
RF voltage (MV)	1.23
RF frequency at injection (MHz)	37.9
RF frequency at extraction (MHz)	53.0
Protons per bunch	3×10^{11}
Harmonic number	84
Total number of protons	2.5×10^{13}
Normalized transverse emittance (mm-mrad)	50π
Longitudinal emittance (eV-sec)	0.03
RF frequency (MHz)	53
γ_{tr} (GeV)	$26i$ or 26
Acceleration time (s)	3.7982×10^{-2}
Beam radius (m) at 400 MeV	3.84×10^{-2}
Beam radius (m) at 8.98 GeV	1.255×10^{-2}
Pipe radius (m)	0.05
Impedance $Z_{\|\|}/n$ (Ω)	5
Beam pipe cutoff frequency (Hz)	1.75819×10^{9}

TABLE III. Resonance table values used to model broadband impedance in ESME simulations.

Energy (GeV)	Shunt Impedance (Ω)
0.4	1.9487395×10^4
4.351591	1.4230288×10^4
8.982666	1.3972×10^4
13.65060	1.39285×10^4